Rigorous theoretical derivation of lumped models to transmission line systems*

Zhao Jixiang(赵吉祥)†

Department of Electronic and Communication Engineering, China Jiliang University, Hangzhou 310018, China

Abstract: By virtue of the negative electric parameter concept, i.e. negative lumped resistance, inductance, conductance and capacitance (N-RLGC), the lumped equivalent models of transmission line systems, including the circuit model, two-port π-network and T-network, are given. We start from the N-segment-ladder-like equivalent networks composed distributed parameters, and achieve the input impedance in the form of a continued fraction. Utilizing the continued fraction theory, the expressions of input impedance are obtained under three kinds of extreme cases, i.e. the load impedances are equal to zero, infinity and characteristic impedance, respectively. When the number of segment N is limited to infinity, they are transformed to lumped elements. Comparison between the distributed model and lumped model of transmission lines, the expression of $\tanh \gamma d$, which is the key term in the transmission line equations, are obtained by RLGC, furthermore, according to input admittance, admittance matrix and ABCD matrix of transmission lines, the lumped equivalent circuit models, π-networks and T-networks have been given. The models are verified in the frequency and time domain, respectively, showing that the models are accurate and efficient.

1. Introduction

Transmission lines (TLs) are widely used in silicon-based radio-frequency (RF) integrated circuits (ICs), due to their low cost and ease of process integration. With the continuous increase of operating frequencies of very large scale integrated circuits, the analog behavior of global digital interconnects becomes more important, whereas for analog design, accurate transmission line models are required to be able to quantify interconnect signal delay and loss[1]. TLs can be modeled by a cascade of equivalent circuits, consisting of series inductances and shunt capacitances with loss resistances and conductances, as shown in Fig. 1. For this circuit, two more aspects must be taken into account. They require a large number of elements and internal nodes to be accurate, resulting in large memory consumption and long simulation time[2]. Furthermore, as the number of nodes increases, the accumulation of rounding errors increase[3].

The negative capacitance effect (NCE) and negative resistance effect (NRE) have been displayed by a variety of electronic devices, with both heterostructures and homostructures. It was verified that in many cases the NCE and NRE phenomena were caused by contact or interface effects[4−6]. The NCE and NRE may occur to a transmission line system, such as a microstrip line.

Thus by virtue of the concept of N-RLGC, this paper gives new lumped equivalent circuit models, π-networks and T-networks of transmission lines, which compose the lumped RLGC elements. The process of deducing and modeling is given, accuracy is verified by frequency, and the time domain is given.

2. Modeling transmission lines

2.1. Input impedance of transmission lines

Let $x = (R + sL)/N$, $y = N/(G + sC)$ in Fig. 1, where R, L, G and C represent the total resistance, inductance, conductance and capacitance of a transmission line. Z_L is the load impedance, N is the number of segments, $s = j\omega$ and ω is the angle frequency. Then the input impedance of the first segment is

$$Z_1 = x + \frac{yZ_L}{y + Z_L} = x + \frac{1}{\dfrac{1}{y} + \dfrac{1}{Z_L}}.$$

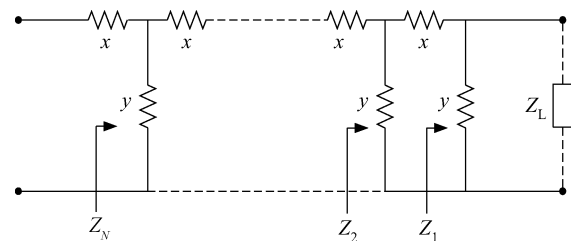Dividing both sides of the above equation by $\sqrt{xy}$ and getting the reciprocal gives

Fig. 1. Transmission line model by ladder networks, $x = (R + sL)/N$, $y = N/(G + sC)$.

$$\frac{\sqrt{xy}}{Z_1} = \cfrac{1}{\sqrt{\frac{x}{y}} + \cfrac{1}{\sqrt{\frac{x}{y}} + \cfrac{1}{\frac{Z_L}{\sqrt{xy}}}}}.$$

Similarly, one can obtain the total input impedance of transmission lines as

$$\frac{\sqrt{xy}}{Z_N} = \cfrac{1}{\sqrt{\frac{x}{y}} + \cfrac{1}{\sqrt{\frac{x}{y}} + \cfrac{1}{\ddots \sqrt{\frac{x}{y}} + \cfrac{1}{\frac{Z_L}{\sqrt{xy}}}}}}. \quad (1)$$

In Eq. (1), the continued fraction includes a $2N$ unit of $\sqrt{x/y}$. Let the hyperbolic function $\sinh\theta = 0.5\sqrt{x/y}$, then three kinds of extreme cases are given as follows[7].

(1) When $Z_L \to \infty$,

$$Z_{N\text{-open}} = \sqrt{xy}\frac{\cosh(2N+1)\theta}{\sinh 2N\theta}. \quad (2)$$

(2) When $Z_L \to 0$

$$Z_{N\text{-short}} = \sqrt{xy}\frac{\sinh 2N\theta}{\cosh(2N-1)\theta}. \quad (3)$$

(3) When $Z_L = Z_0$, where Z_0 is the characteristic impedance of transmission lines, using $1/(1+x) \approx 1-x$, yields

$$Z_{N\text{-ch}} = \sqrt{xy} = \sqrt{\frac{R+sL}{G+sC}} = Z_0,$$

by De Moiver's formula $(\cosh x \pm \sinh x)^m = \cosh mx \pm \sinh mx$ and $(1 \pm x)^m \approx 1 \pm mx + 0.5m(m-1)x^2 \pm m(m-1)(m-2)x^3/3! + \cdots$ [8], one can obtain

$$\cosh m\theta = 0.5[(\cosh\theta + \sinh\theta)^m + (\cosh\theta - \sinh\theta)^m]$$

$$= 0.5\left\{\left[\sqrt{1+\frac{1}{4}\frac{x}{y}} + \frac{1}{2}\sqrt{\frac{x}{y}}\right]^m + \left[\sqrt{1+\frac{1}{4}\frac{x}{y}}\right.\right.$$

$$\left.\left. -\frac{1}{2}\sqrt{\frac{x}{y}}\right]^m\right\}$$

$$\approx \left[\sqrt{1+\frac{1}{4}\frac{x}{y}}\right]^m \times$$

$$\left[1 + \frac{m(m-1)}{2}\left(\frac{1}{2}\sqrt{\frac{x}{y}}/\sqrt{1+\frac{1}{4}\frac{x}{y}}\right)^2 + \cdots\right].$$

$$(4)$$

$$\sinh m\theta = \frac{1}{2}[(\cosh\theta + \sinh\theta)^m - (\cosh\theta - \sinh\theta)^m]$$

$$= \frac{1}{2}\left\{\left[\sqrt{1+\frac{1}{4}\frac{x}{y}} + \frac{1}{2}\sqrt{\frac{x}{y}}\right]^m - \left[\sqrt{1+\frac{1}{4}\frac{x}{y}}\right.\right.$$

$$\left.\left. -\frac{1}{2}\sqrt{\frac{x}{y}}\right]^m\right\}$$

$$\approx \left[\sqrt{1+\frac{1}{4}\frac{x}{y}}\right]^m \times$$

$$\left[\frac{m}{2}\sqrt{\frac{x}{y}}/\sqrt{1+\frac{1}{4}\frac{x}{y}} + \frac{m(m-1)(m-2)}{3!}\right.$$

$$\left. \times \left(\frac{1}{2}\sqrt{\frac{x}{y}}/\sqrt{1+\frac{1}{4}\frac{x}{y}}\right)^3 + \cdots\right].$$

$$(5)$$

Substitute into Eqs. (2) and (3), they expand to

$$Z_{N\text{-open}} = \sqrt{xy}\frac{\cosh(2N+1)\theta}{\sinh 2N\theta}$$

$$\approx \frac{1}{G+sC}\frac{1+(R+sL)(G+sC)/2}{1+(R+sL)(G+sC)/6}, \quad N \to \infty,$$

$$(6)$$

$$Z_{N\text{-short}} = \sqrt{xy}\frac{\sinh 2N\theta}{\cosh(2N-1)\theta}$$

$$\approx (R+sL)\frac{(R+sL)(G+sC)/6}{1+(R+sL)(G+sC)/2}, \quad N \to \infty.$$

$$(7)$$

2.2. Equivalent circuit for transmission lines

The input impedance and admittance of a distributed model to lossy transmission lines are

$$Z_{\text{in}} = Z_0\frac{Z_L + Z_0\tanh\gamma d}{Z_0 + Z_L\tanh\gamma d}, \quad (8)$$

$$Y_{\text{in}} = \frac{1}{Z_0}\frac{Z_0 + Z_L\tanh\gamma d}{Z_L + Z_0\tanh\gamma d}, \quad (9)$$

where γ and d are the propagation constant, and the total length of the transmission line, respectively. The open- and short-circuited impedance are given

$$Z_{\text{open}} = \frac{Z_0}{\tanh\gamma d}, \quad (10)$$

$$Z_{\text{short}} = Z_0\tanh\gamma d. \quad (11)$$

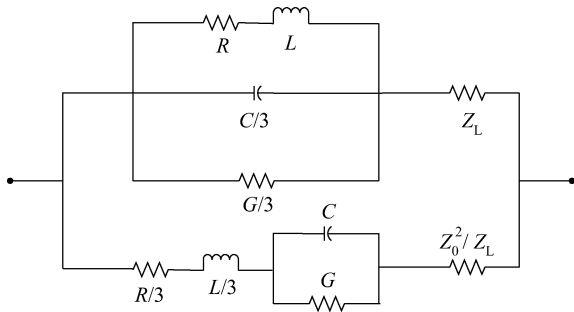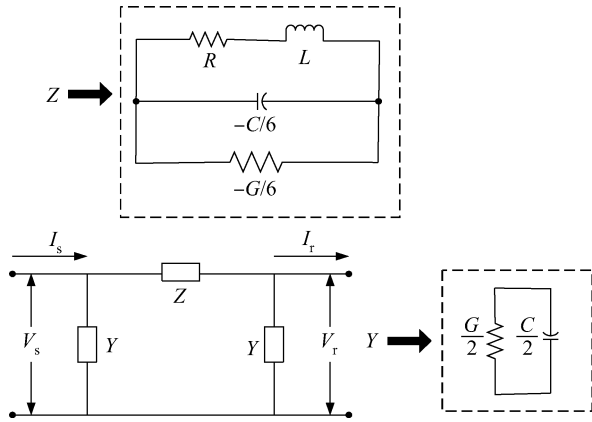In comparison with Eqs. (6) and (10), (7) and (11), respectively, identical results are obtained.

Fig. 2. Equivalent circuit of Eq. (10).

Fig. 3. Frame and lumped element π-network of transmission lines.

$$\tanh \gamma d = \sqrt{(R + sL)(G + sC)}\frac{1 + (R + sL)(G + sC)/6}{1 + (R + sL)(G + sC)/2}.$$

$$(12)$$

And then

$\sinh \gamma d$

$$\approx \frac{\sqrt{(R + sL)(G + sC)}}{1 - (R + sL)(G + sC)/6 + [(R + sL)(G + sC)]^2/48}.$$

$$(13)$$

Using Eqs. (9) and (12), we obtain the input admittance:

$$Y_{\text{in}}(s) \approx \cfrac{1}{Z_{\text{L}} + \cfrac{R + sL}{1 + (R + sL)(G + sC)/3}}$$

$$+ \cfrac{1}{\cfrac{Z_0^2}{Z_{\text{L}}} + \cfrac{1 + (R + sL)(G + sC)/3}{G + sC}}. \qquad (14)$$

According to Eq. (14), the corresponding equivalent circuit is shown in Fig. 2.

2.3. Equivalent π-networks for transmission lines

The distributed transmission line equations are

$$V_{\text{s}} = V_{\text{r}} \cosh \gamma d + I_{\text{r}} Z_0 \sinh \gamma d, \qquad (15)$$

Fig. 4. Frame and lumped element T-networks of transmission lines.

$$I_{\text{s}} = V_{\text{r}}\frac{\sinh \gamma d}{Z_0} + I_{\text{r}} \cosh \gamma d. \qquad (16)$$

The π-network frame is shown in Fig. 3, it produces[9]

$$V_{\text{s}} = (1 + ZY)V_{\text{r}} + ZI_{\text{r}}, \qquad (17)$$

$$I_{\text{s}} = (2Y + ZY^2)V_{\text{r}} + (1 + ZY)I_{\text{r}}, \qquad (18)$$

where V_{s}, V_{r}, and I_{s}, I_{r} are sending- or receiving-end voltages and currents, Z and Y are resistance and admittance, respectively.

Comparing Eqs. (15), (17) and Eqs. (16), (18), and utilizing Eq. (9), one obtains

$$Z = Z_0 \sinh \gamma d \approx \cfrac{R + sL}{1 - \cfrac{(R + sL)(G + sC)}{6}}$$

$$= \frac{-6(R + sL)/(G + sC)}{(R + sL) - 6/(G + sC)}. \qquad (19)$$

$$Y = \frac{1}{Z_0} \tanh(\gamma d/2) = \frac{1}{Z_0}\left(\frac{1}{\tanh \gamma d} - \frac{1}{\sinh \gamma d}\right)$$

$$\approx 0.5(G + sC). \qquad (20)$$

From Eqs. (19) and (20), by virtue of the concept of N-RLGC, equivalent π-networks are obtained and depicted in Fig. 3.

2.4. Equivalent T-networks for transmission lines

The ABCD matrices of distributed parameters and lumped elements from the T-network (depicted in Fig. 4) of transmission lines are listed as below[10], respectively,

$$[A_{\text{distributed}}] = \begin{bmatrix} \cosh \gamma d & Z_0 \sinh \gamma d \\ \sinh \gamma d / Z_0 & \cosh \gamma d \end{bmatrix}, \qquad (21)$$

$$[A_{\text{lumped}}] = \begin{bmatrix} 1 + \dfrac{Z_1}{2Z_2} & Z_1 + \dfrac{Z_1^2}{4Z_2} \\ \dfrac{1}{Z_2} & 1 + \dfrac{Z_1}{2Z_2} \end{bmatrix}. \qquad (22)$$
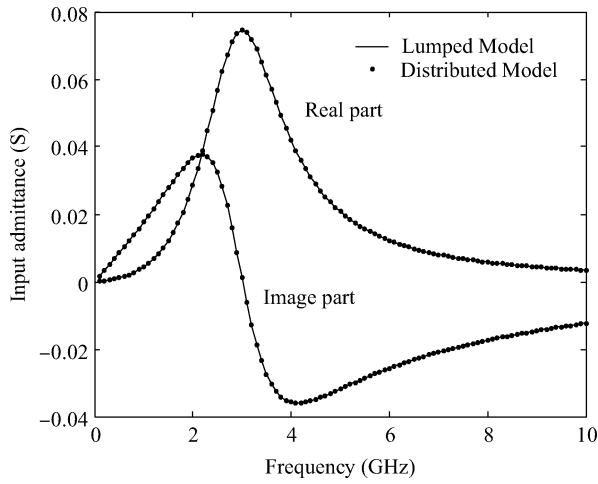
Fig. 5. Input admittance with a capacitive load $C_L = 500$ fF, the maximal relative errors of real and image part are 1.19% and 0.63%, respectively.
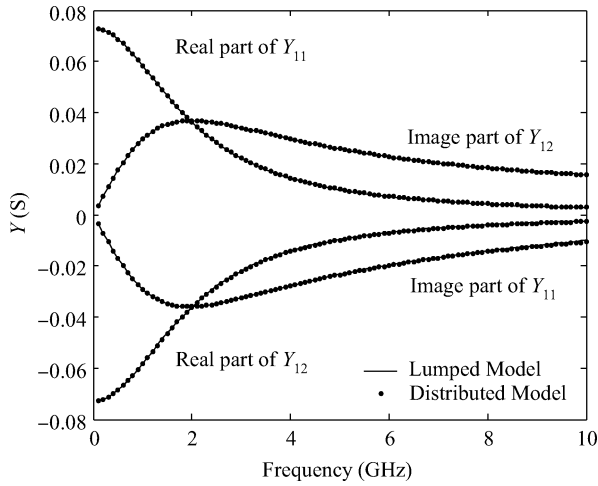

Fig. 6. Y parameters of π-networks versus frequency, the maximal relative errors of real and image part are (1) Y_{11}: 5.21%, 0.70%; (2) Y_{12}: 0.53% and 1.96%, respectively.

Comparing Eqs. (21) and (22), one can obtain

$$\frac{Z_1}{2} \approx \frac{R + sL}{2} - \frac{(R + sL)^2(G + sC)}{24}$$

$$\approx \frac{\dfrac{R + sL}{2} \dfrac{6}{G + sC}}{\dfrac{R + sL}{2} + \dfrac{6}{G + sC}}, \tag{23}$$

$$Z_2 \approx \frac{1}{G + sC} - \frac{R + sL}{6} + \frac{(R + sL)^2(G + sC)}{48}$$

$$\approx \frac{1}{G + sC} + \frac{\left(-\dfrac{R + sL}{6}\right)\left(-\dfrac{4/3}{G + sC}\right)}{\left(-\dfrac{R + sL}{6}\right) + \left(-\dfrac{4/3}{G + sC}\right)}, \tag{24}$$

by introducing N-RLGC, an analytical lumped T-network of transmission lines is depicted in Fig. 4.
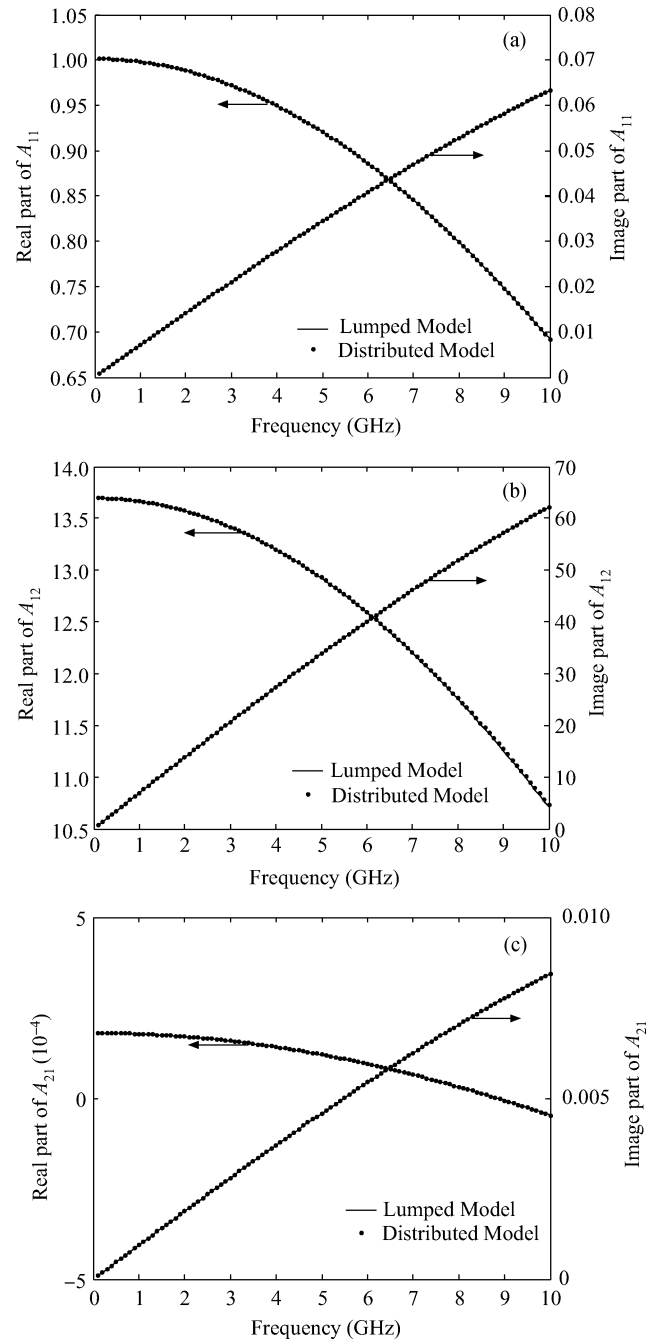

Fig. 7. ABCD parameters from Fig. 4 versus frequency. (a) A_{11} versus frequency, the maximal relative errors are 0.03% (real part) and 0.02% (image part) (b) A_{12} versus frequency, the maximal relative errors are 0.05% (real part) and 0.02% (image part) (c) A_{21} versus frequency, the maximal relative errors are 0.01% (real part) and 0.01% (image part)

3. Model verification

3.1. Frequency domain verification

3.1.1. Input admittance

In order to verify the utilized algorithm, the distributed model from Eq. (9) and the lumped model from Eq. (14) are compared. The IC technology cross section is shown in Fig. 2 of Ref. [11] and parameters are chosen from Ref. [11], i.e. $r = 136.9$ Ω/cm, $l = 11.0$ nH/cm, $c = 1.5$ pF/cm, $g =$

1.8×10^{-3} S/cm, and the length of transmission lines $d = 1$ mm, the approximate lumped parameters are $R = rd, L = ld$, $C = cd$, and $G = gd$, the driver resistance $R_{th} = 20\ \Omega$, and load resistance Z_L is a capacitive load and its capacitance $C_L = 500$ fF. The simulation result is presented in Fig. 5.

3.1.2. π-networks

The admittance matrix from the equivalent π-network (Fig. 3) is

$$[Y_{\text{net}}] = \begin{bmatrix} Y + \dfrac{1}{Z} & -\dfrac{1}{Z} \\ -\dfrac{1}{Z} & Y + \dfrac{1}{Z} \end{bmatrix}. \quad (25)$$

And the admittance matrix of the distributed model of transmission lines is

$$[Y_{\text{exact}}] = \dfrac{1}{Z_0} \begin{bmatrix} \coth \gamma d & -\csc \gamma d \\ -\csc \gamma d & \coth \gamma d \end{bmatrix}. \quad (26)$$

The same parameters are chosen as for Section 3.1, Y_{11} and Y_{12} are depicted in Fig. 6.

3.1.3. T-networks

The validity and accuracy of T-networks are evaluated through parameters A_{11}, A_{12}, A_{12} of the ABCD matrix of transmission lines in the frequency domain. The transmission line parameters are the same as above. The simulation results from the distributed model and the lumped model are presented in Fig. 7.

3.2. Time domain verification

A single RLCG line proposed in Refs. [12, 13] is considered. The lossy transmission line with load capacitance $C_L = 500$ fF is 1 cm long, and its parameters are $R = 42.5\ \Omega, C = 1.1$ pF, $L = 4.05$ nH and $G = 0.3$ mS, and the driver resistance $R_s = 23.54\ \Omega$. The input signal is a ramp with a rise time of 0.1 ns and voltage 1.2 V. The near- and far-end response is discussed in this section.

3.2.1. The near-end response

The transfer function from the input to the near-end is

$$H_{\text{near}}(s) = \frac{V_{\text{out-near}}(s)}{V_{\text{in}}(s)} = \frac{Z_{\text{in}}(s)}{Z_{\text{in}}(s) + R_s} = \frac{1}{1 + Y_{\text{in}}(s)R_s}$$

$$= \frac{b_2 s^2 + b_1 s + b_0}{s^3 + a_2 s^2 + a_1 s + a_0} = \frac{b_2 s^2 + b_1 s + b_0}{(s - s_1)(s - s_2)(s - s_3)}, \quad (27)$$

where s_1, s_2 and s_3 are the roots of the equation $s^3 + a_2 s^2 + a_1 s + a_0 = 0$. Their analytical formulas can be obtained by the Gerolamo Cardano method[8], and the other parameters are given as follows:

$$a_0 = \frac{3 + RG + 3R_s G}{LCR_s C_L},$$

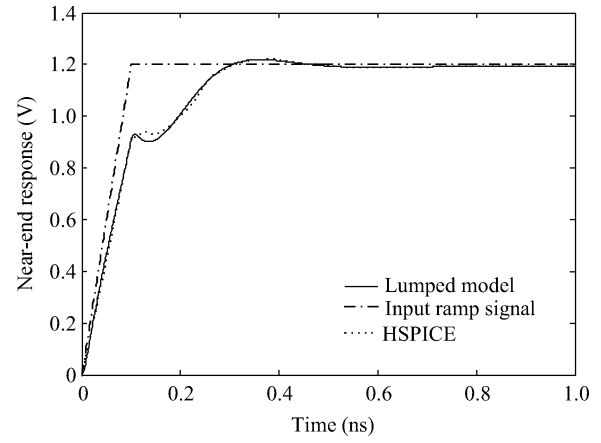$$a_1 = \frac{RC + GL + R_s RG C_L + 3RC_L + 3R_s C_L + 3R_s C}{LCR_s C_L},$$

Fig. 8. Near-end ramp response.

$$a_2 = \frac{LC + 3LC_L + R_s C_L(RC + GL)}{LCR_s C_L},$$

$$b_2 = \frac{LC + 3LC_L}{LCR_s C_L}, \quad b_1 = \frac{RC + GL + 3RC_L}{LCR_s C_L},$$

$$b_0 = \frac{3 + RG}{LCR_s C_L}.$$

In this case, there is one real root (s_1) and two complex conjugated roots (s_2 and s_3), so the inverse Laplace transformation has to follow the form.

$$h_{\text{near}}(t) = A_1 e^{s_1 t}$$
$$+ F\{k_c(B_1, C_1), k_s[B_1, C_1, \omega(s_2, s_3)], \alpha(s_2, s_3)\}, \quad (28)$$

where

$$F\{k_c(x, y), k_s[x, y, \omega(s_m, s_n)], \alpha(s_m, s_n)\}$$
$$= k_c e^{\alpha t} \cos \omega t + k_s e^{\alpha t} \sin \omega t, \quad (29)$$

and

$$k_c(x, y) = x + y, \quad k_s[x, y, \omega(s_m, s_n)] = \frac{(x - y)(s_m - s_n)}{2\omega(s_m, s_n)},$$

$$\alpha(s_m, s_n) = \frac{s_m + s_n}{2}, \quad \omega(s_m, s_n) = \sqrt{s_m s_n - \left(\frac{s_m + s_n}{2}\right)^2},$$

$$A_1 = \frac{b_2 s_1^2 + b_1 s_1 + b_0}{(s_1 - s_2)(s_1 - s_3)}, \quad B_1 = \frac{b_2 s_2^2 + b_1 s_2 + b_0}{(s_2 - s_1)(s_2 - s_3)},$$

$$C_1 = \frac{b_2 s_3^2 + b_1 s_3 + b_0}{(s_3 - s_1)(s_3 - s_2)}.$$

Convoluting $h_{\text{near}}(t)$ with the input ramp signal, the simulation and HSPISE results are depicted in Fig. 8.

3.2.2. The far-end response

The transfer function from the input to the far-end of a line with source and load impedance for a transmission line system can be carried out based on the lumped element π-networks by chain matrix formulation. It is given by

$$H_{\text{far}}(s) = \frac{b_0}{s^4 + a_3 s^3 + a_2 s^2 + a_1 s + a_0}$$

$$= \frac{b_0}{(s - s_1)(s - s_2)(s - s_3)(s - s_4)}. \qquad (30)$$

where s_1, s_2, s_3 and s_4 are the roots of the equation $s^4 + a_3 s^3 + a_2 s^2 + a_1 s + a_0 = 0$. The analytical formulas can be found in Ref. [8]. There are two pairs of complex conjugated roots (s_1, s_2) and (s_3, s_4). The other parameters are given as follows:

$$b_0 = \frac{6}{C C_{\text{L}} L^2},$$

$$a_3 = \frac{C_{\text{L}} G L^2 + L R_{\text{s}} C^2 + 2 C C_{\text{L}} L R + 3 C C_{\text{L}} L R_{\text{s}}}{C C_{\text{L}} L^2},$$

$$a_2 = \frac{C C_{\text{L}} R^2 + C^2 R R_{\text{s}} + 2 C_{\text{L}} G L R + 2 C G L R_{\text{s}}}{C C_{\text{L}} L^2}$$
$$+ \frac{3 C L + 3 C_{\text{L}} G L R_{\text{s}} + 3 C C_{\text{L}} R R_{\text{s}} + 6 L C_{\text{L}}}{C C_{\text{L}} L^2},$$

$$a_1 = \frac{C_{\text{L}} G R^2 + G^2 L R_{\text{s}} + 2 C G R R_{\text{s}}}{C C_{\text{L}} L^2}$$
$$+ \frac{3(G L + C R + C_{\text{L}} G R R_{\text{s}}) + 6(C_{\text{L}} R + C R_{\text{s}} + C_{\text{L}} R_{\text{s}})}{C C_{\text{L}} L^2},$$

$$a_0 = \frac{6 + G^2 R R_{\text{s}} + 3 G R + 6 G R_{\text{s}}}{C C_{\text{L}} L^2}.$$

The inverse Laplace transformation is

$$h_{\text{far}}(t) = F\{k_{\text{c}}(B_2, A_2), k_{\text{s}}[B_2, A_2, \omega(s_1, s_2)], \alpha(s_1, s_2)\}$$
$$+ F\{k_{\text{c}}(D_2, C_2), k_{\text{s}}[D_2, C_2, \omega(s_3, s_4)], \alpha(s_3, s_4)\}, \qquad (31)$$

$$A_2 = \frac{b_0}{(s_1 - s_2)(s_1 - s_3)(s_1 - s_4)},$$

$$B_2 = \frac{b_0}{(s_2 - s_1)(s_2 - s_3)(s_2 - s_4)},$$

$$C_2 = \frac{b_0}{(s_3 - s_1)(s_3 - s_2)(s_3 - s_4)},$$

$$D_2 = \frac{b_0}{(s_4 - s_1)(s_4 - s_2)(s_4 - s_3)}.$$

Similarly, convoluting $h_{\text{far}}(t)$ with the input ramp signal, the simulation and HSPISE results are depicted in Fig. 9.
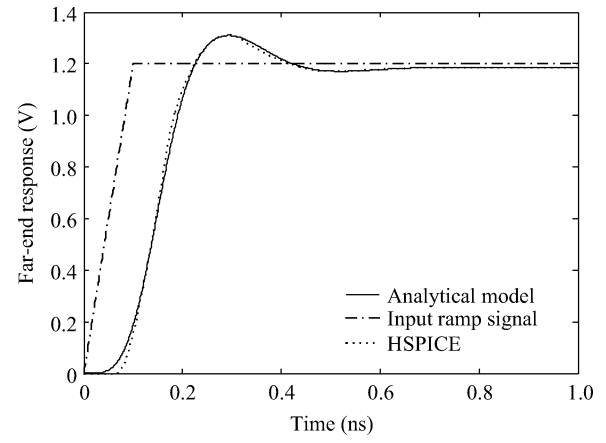

Fig. 9. Far-end ramp response.

4. Discussion and summary

Based on continued fraction theory and by virtue of the N-RLGC, the lumped elements equivalent circuits of transmission lines are given and compared with the distributed model. The errors are given in the caption of each figure. For Figs. 5 and 6, the maximal relative error is 5.21%, and for Fig. 7, the maximal relative error is 0.05%. The reasons for the relatively large difference between the errors are that second order approximation of series $(1 + x)^m$ is adopted in Eqs. (14), (19), and (20), and third order approximation in Eqs. (23) and (24), respectively. The simulated near- and far-end response of the ramp signal is compared with HSPICE with a mean relative error of less than 2%, so this equivalent network is accurate.

To equivalent circuits, π-networks and T-networks, all errors come from three areas: first, the approximate hyperbolic tangent and sine expression from Eqs. (12) and (13); second, the disregard of end- or fringe-effects of transmission lines, and adopting $R = rd$, $L = ld$, $C = cd$, and $G = gd$ instead of the total resistance, inductance, conductance and capacitance of transmission lines; last, these parameters are taken to be constant, although they are often frequency dependent (e.g., due to the skin effect).

5. Conclusion

The lumped models, π-networks and T-networks of transmission lines are given in this paper. These models are useful for measuring and extracting the interconnect performance of IC interconnect conductors and dielectrics in a single. As a necessary tool for circuit design, it can efficiently represent their electrical performance for circuit simulation with other design components.

References

[1] Tiemeijer L F, Pijper R M T, Noort W V. On the accuracy of the parameters extracted from S-parameter measurements taken on differential IC transmission lines. IEEE Trans Microw Theory Tech, 2009, 57(6): 1581

[2] Kallio A, Veijola T. Synthesis of reduced equivalent circuits for transmission lines. IEEE Trans Circuits Syst I, Reg Papers, 2006,

53(10): 2255

[3] Antonini G, Ferri G. Compact transmission line representation. IEE Proc Sci Meas Technol, 2004, 151(3): 211

[4] Rahaman M S, Chowdhury M H. Interconnect technique for sub-threshold circuits using negative capacitance effect, circuits and systems. 52nd IEEE International Midwest Symposium on MWSCAS, 2009

[5] Ershov M, Liu H C, Li L, et al. Negative capacitance effect in semiconductor devices. IEEE Trans Electron Devices, 1998, 45(10): 2196

[6] Yuan J H, Cressler J D, Zhu C D, et al. An investigation of negative differential resistance and novel collector-current kink effects in SiGe HBTs operating at cryogenic temperatures. IEEE Trans Electron Devices, 2007, 54(3): 504

[7] Yan X J. Hyperbolic functions theory. China Science & Technology Press, 1957: 32

[8] The groups of handbook of mathematics. Handbook of mathematics. China Higher Education Press, 1979

[9] Indulkar C S, Ramalingam K. Estimation of transmission lines parameters from measurements. Electrical Power and Energy Systems, 2008, 30(5): 337

[10] Ludwig R, Bretchko P. RF circuit design: theory and application. Beijing: Publishing House of Electronics Industry, 2002

[11] Eisenstadt W R, Eo Y. S-parameter-based IC interconnect transmission line characterization. IEEE Trans Compon Hybrids Manufact Technol, 1992, 15(4): 483

[12] Venkatesan R, Davis J A, Meindl J D. Compact distributed RLC interconnect models—part III: transients in single and coupled lines with capacitive load termination. IEEE Trans Electron Devices, 2003, 50(4): 1081

[13] Kang K, Yin W Y, Li L W. Transfer functions of on-chip global interconnects based on distributed RLCG interconnects model. IEEE Antennas and Propagation Society International Symposium, Washington, July 2005, 1A: 524